Electronic Supplementary Material (ESI) for ChemComm.

Supplementary Information

Low-defect $K_2Mn[Fe(CN)_6]$-reduced graphene oxide composite for high-performance potassium-ion batteries

Juan Zhang, † [a] Leqing Deng, † [a,b], Meiying Feng, [a] Liang Zeng,[c] Miao Hu,[d] and Yujie Zhu *[a,e]

[a] School of Chemistry, Beihang University, Beijing 100191, P. R. China. Email: yujiezhu@buaa.edu.cn Address here.
[b] School of Physics, Beihang University, Beijing 100191, P. R. China.
[c] Key Laboratory for Green Chemical Technology of Ministry of Education, School of Chemical Engineering and Technology, Collaborative Innovation Center of Chemical Science and Engineering, Tianjin University, Tianjin 300072, P. R. China.
[d] CNOOC Research Institute of Refining and Petrochemicals, Beijing 102200, P. R. China.
[e] Beijing Advanced Innovation Center for Biomedical Engineering, Beihang University, Beijing 100191, P. R. China.
†*Authors contributed equally to this work.*

Experimental Section

1. Materials Synthesis

All the reagents used in this work are commercially available and used as-received. The $K_2MnFe(CN)_6$ (KMF) sample was obtained *via* a simple chelating agent assisted precipitation method. Typically, the KMF sample was fabricated under room temperature as follows: 1) 2 mmol of trans-1,2-cyclohexanediaminetetraacetic acid (CyDTA, Aladdin) and 2 mmol of KOH (Beijing Chemical Works) were mixed in 50 mL of deionized water and stirred to get a clear solution (marked as solution A); 2) then, 2 mmol of $Mn(CH_3COO)_2{\cdot}4H_2O$ (Aladdin) was dissolved in solution A to obtain the solution B; 3) afterwards, the solution B was dropwise added into 50 mL solution containing 2 mmol $K_4Fe(CN)_6{\cdot}3H_2O$ (Aladdin) with continuous magnetic stirring and N_2 bubbling. The resulting precipitate was collected by centrifugation, washed with water, and dried under vacuum at 80 ˚C for 12 h. The KMF-RGO sample was prepared by ball milling the mixture of KMF (70 wt.%) and reduced graphene oxide (RGO, 10 wt.%, Qiaihe Baotailong) at 1200 rpm for 2 h with a ball: powder mass ratio of 20:1.

2. Materials Characterizations

The X-ray diffraction (XRD) spectra were collected using a Rigaku Dmax-2200 from 10 degree to 60 degree with Cu Kα radiation (λ = 1.5416 Å). Fourier transform infrared (FT-IR) spectra were recorded by the FT-IR Microscope (Nicolet iN10). Thermal gravimetric analysis (TGA) measurement was conducted on a NETZSCH STA 449 F5/F3 instrument with a heating rate of 10 °C min^{-1} under N_2 flow from room temperature to xx ˚C. X-ray photoelectron spectroscopy (XPS) characterizations were carried out with a Thermo Escalab 250Xi with Al Kα (hv = 1486.6 eV) X-ray radiation and all binding energies of the XPS spectra were corrected by referencing C 1s to 284.8 eV. Inductively coupled plasma mass spectrometry (ICP-MS) data were measured by an Agilent ICPMS7800. The morphologies were recorded on a field emission scanning electron microscope (JEOL, JSM-7500F, 5kV). UV-vis spectra were collected by a UV-2700 (Shimadzu, Japan).

3. Electrochemical Measurements

KMF- RGO (80 wt.%), Ketjen Black (KB, 10 wt.%), and polyvinylidene fluoride (PVDF, 10 wt.%) were dissolved in N-methyl-2-pyrrolidone to form a slurry, which was coated on aluminum foil (16 um, MTI Corp.) to obtain the working electrode, and then dried in vacuum at 80 °C for overnight. For the electrochemical tests in Figure 2 and S3, the areal loading of KMF-RGO on the electrode was around 4 mg cm^{-2}. For other electrochemical tests, a relatively low areal loading of 1 mg cm^{-2} of KMF was used. The graphite anode was prepared by coating graphite, KB and PVDF on copper foil with a weight ratio of 8:1:1. Half-cells (coin-type, 2032, MTI Corp.) were assembled in an argon-filled glove box with both water and oxygen content less than 0.1 ppm by using working electrode, potassium metal as counter electrode, glass fiber as separator (Whatman, Grade GF/D) and 2.5 M potassium bis(fluorosulfonyl) imide (KFSI) dissolved in triethyl phosphate (TEP) as the electrolyte,[1] respectively. The galvanostatic charge-discharge tests were performed on the Land battery system (Wuhan LAND electronics, China) at room temperature. Rate capability of the KMF-RGO composite is assessed under a constant charge current density of 0.03 A/g (~ 0.2C) but various discharge rates. In the graphite || KMF- RGO full-cell, both the KMF-RGO cathode and graphite anode were not pre-cycled but directly assembled in the full-cell, and the capacity ratio of anode to cathode is 0.8:1. For the galvanostatic charge-discharge test of the full-cell, the specific current is calculated based on the weight of KMF in the full-cell. The specific energy of the full-cell is calculated by integration of voltage with the specific capacity which is automatically done by the Land battery testing system.

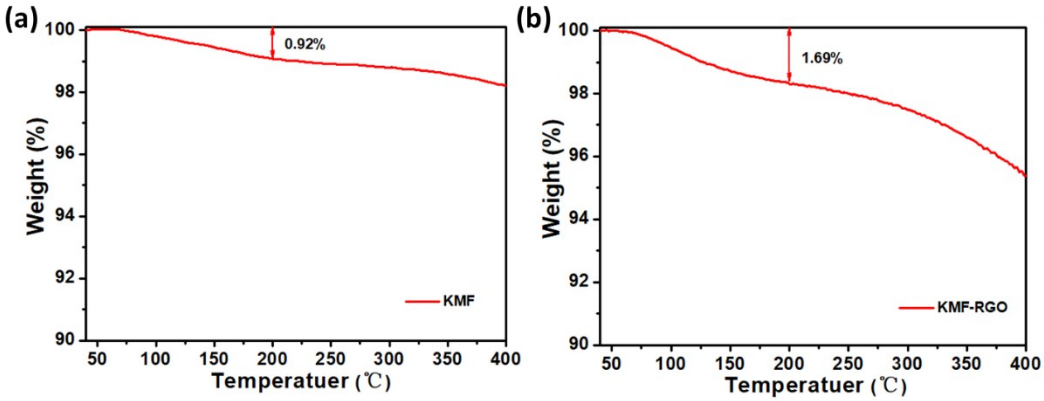

Figure S1. TGA curves of the KMF (a) and (b) KMF-RGO.

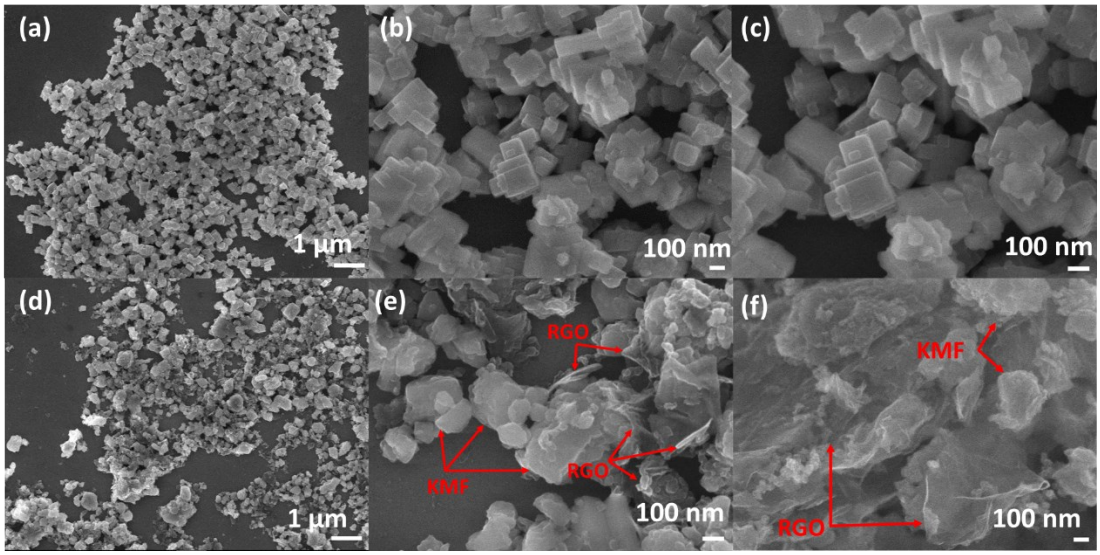

Figure S2. SEM images of (a, b and c) KMF and (d, e and f) KMF-RGO. The RGO and KMF are marked by red arrows in e and f.

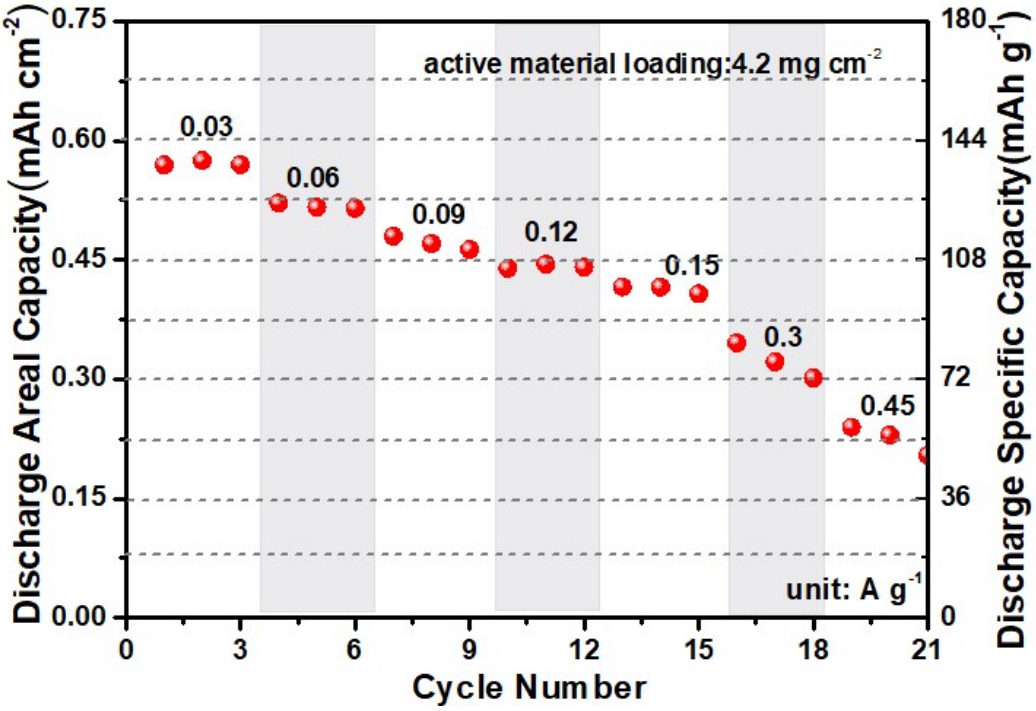

Figure S3. Rate capability of the KMF-RGO electrode with a high loading. The test is done under a constant charge current density of 0.03 A/g (~ 0.2C) but various discharge rates.

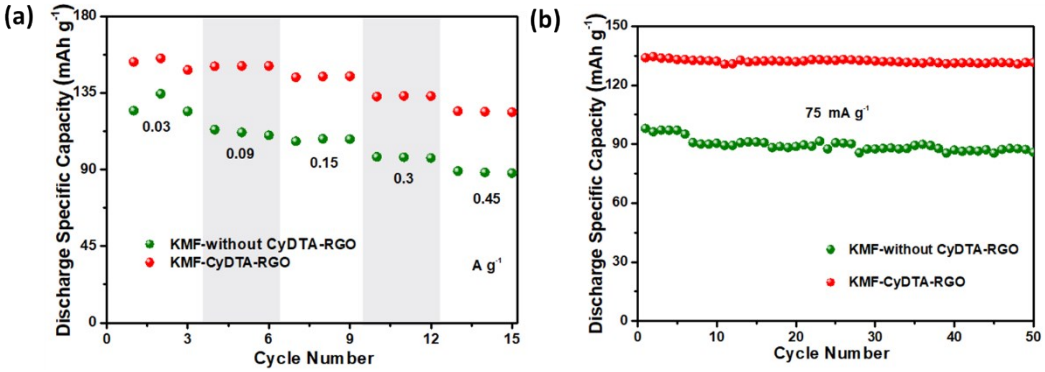

Figure S4. Comparison of (a) rate capability and (b) cycling performance between the KMF-RGO composite synthesized with and without CyDTA. The rate capability test is performed under a constant charge current density of 0.03 A/g (~ 0.2C) but various discharge rates, and the cycling performance test is done under a specific current of 75 mA g^{-1}.

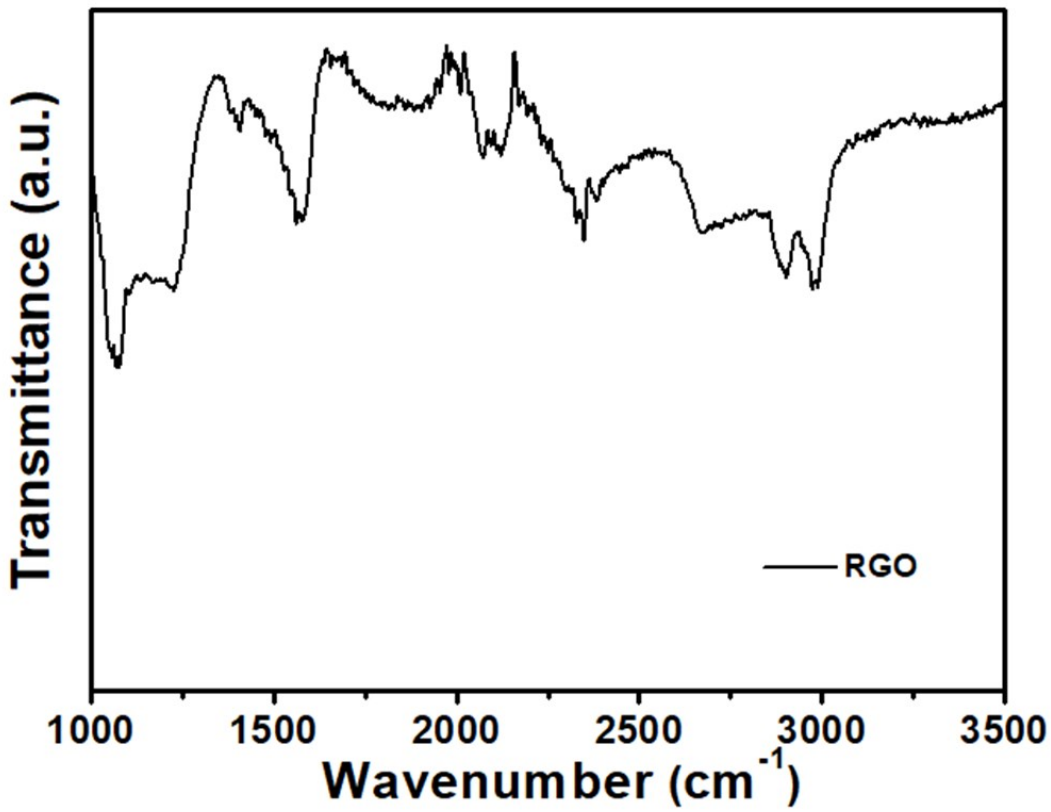

Figure S5. FT-IR spectrum of RGO.

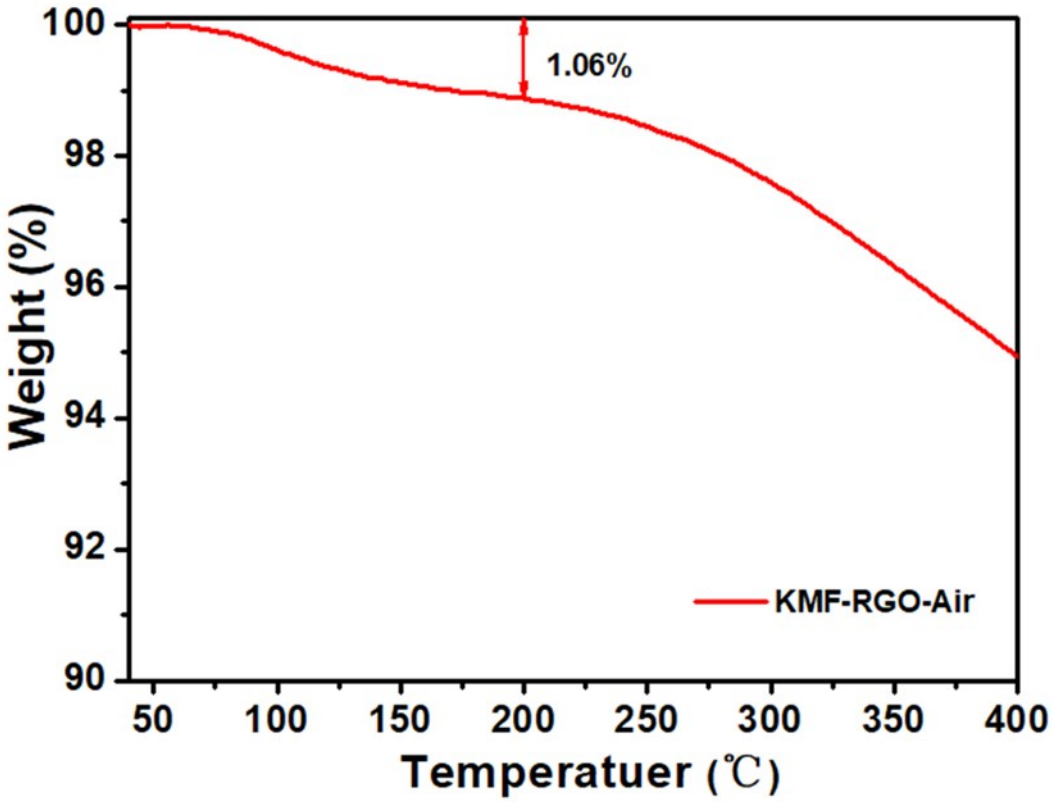

Figure S6. TGA curve of the KMF-RGO-Air sample.

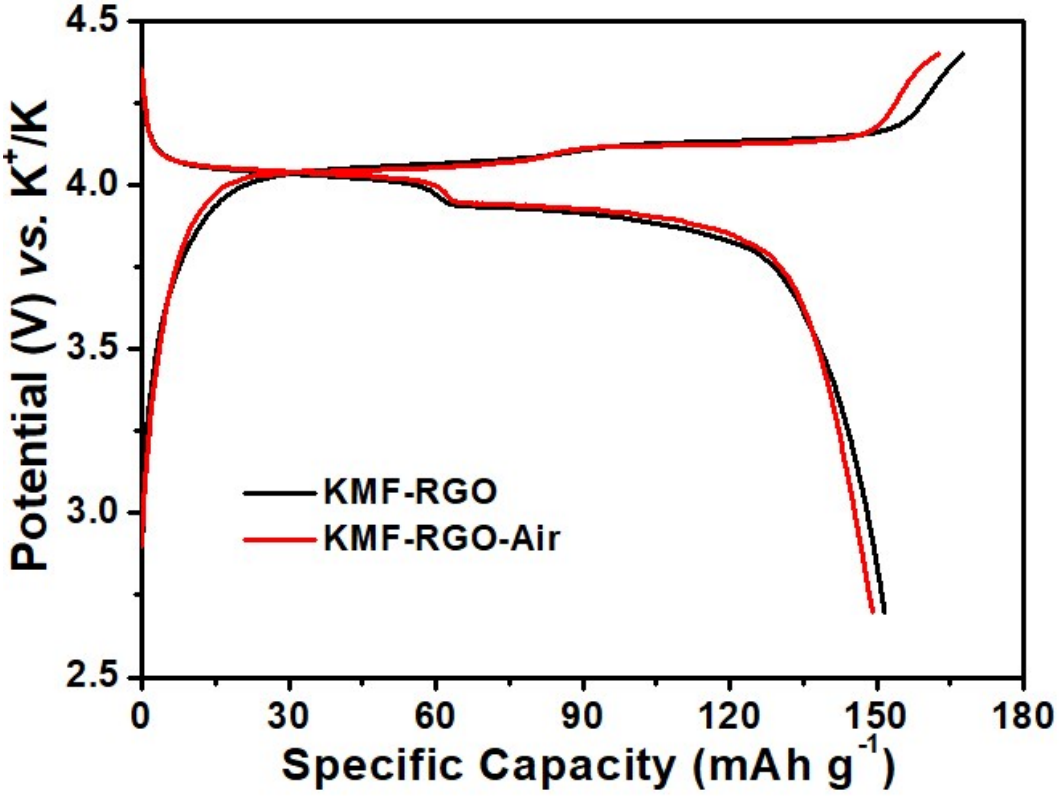

Figure S7. Charge–discharge potential profiles of the KMF-RGO and KMF-RGO-Air at 15 mA g^{-1}.

Table S1. ICP-MS results for the KMF and KMF-RGO

sample	K:Mn:Fe	molecular formula
KMF	2:1:0.982	$K_2Mn[Fe(CN)_6]_{0.982}\square_{0.018}\bullet 0.164H_2O$
KMF-RGO	1.91:1:0.965	$K_{1.91}Mn[Fe(CN)_6]_{0.965}\square_{0.035}\bullet 0.389H_2O$

Table S2. Comparison of the areal capacity for some reported cathode materials for KIBs

.

Cathodes	Discharge capacity (mAh g^{-1}) @Current density (mA g^{-1})	The loading mass of active material（mg cm^{-2}）	areal capacity（mAh cm^{-2}）
$K_{1.91}Mn[Fe(CN)_6]_{0.965}\square_{0.035}\bullet 0.389H_2O$ (This work)	151.8@15	4.2	0.62
$K_{1.94}Mn[Fe(CN)_6]_{0.994}\square_{0.006}\bullet 0.08H_2O$[2]	154.7@15	1	0.15
$K_{1.84}Ni[Fe\ (CN)_6]0.88\cdot 0.49H_2O$[3]	62.8@100	1.5	0.09
$K_2NiFe(CN)_6\cdot 1.2H_2O$[4]	77.4@400	2	0.15
$K_{1.88}Zn_{2.88}[Fe(CN)_6]_2(H_2O)_5$[5]	64.9@69.08	0.84	0.05
$K_2Fe^{II}[Fe^{II}(CN)_6]\cdot 2H_2O$[6]	120@200	2	0.24
$K_{1.93}Fe[Fe(CN)_6]_{0.97}\cdot 1.82H_2O$[7]	142@75	1.015	0.15
$K_{0.220}Fe[Fe(CN)_6]_{0.805}\cdot 4.01H_2O$[8]	73.2@50	0.9	0.07
$K_{1.7}Fe[Fe(CN)_6]_{0.9}$[9]	140@10	0.875	0.12
$K_{1.4}Fe_4[Fe(CN)_6]_3$[10]	71@50	1.05	0.07
$K_{1.85}Mn[Fe(CN)_6]_{0.98}\square_{0.02}\cdot 0.7H_2O$[11]	142.6@15	2.5	0.36
$K_{1.87}Fe[Fe(CN)_6]_{0.97}\cdot\square_{0.03}\cdot 0.84H_2O$[12]	88.9@50	1.68	0.15
$FeFe(CN)_6$[13]	121@62.5	1.2	0.15
$K_{1.6}Mn[Fe(CN)_6]_{0.96}$[14]	115@20	1.6	0.18
$KFe[Fe(CN)_6]$[15]	118.7@10	2	0.24
$K_{0.3}Ti_{0.75}Fe_{0.25}[Fe(CN)_6]_{0.95}\cdot 2.8H_2O$[16]	113@100	0.7	0.08
$Fe[Fe(CN)_6]$[17]	123@111	2.88	0.35
$K_{0.12}Fe[Fe(CN)_6]_{0.75}$[18]	215@1000	1	0.22
$K_{1.92}Fe[Fe(CN)_6]_{0.94}\cdot 0.5H_2O$[19]	133@65	1.4	0.19
$K_{1.81}Ni[Fe(CN)_6]_{0.97}\cdot 0.086H_2O$[20]	57@10	1.75	0.10
$K_{0.77}MnO_2\cdot 0.23H_2O$ [21]	134@100	1.5	0.20
$K_{0.5}MnO_2$[22]	106@5	4.4	0.49
$K_{0.6}CoO_2$[23]	80@2	5.408	0.43
$K_{0.69}CrO_2$[24]	100@10	3.5	0.35
$K_{0.65}Fe_{0.5}Mn_{0.5}O_2$[25]	151@20	1.429	0.22
$K_{0.51}V_2O_5$ [26]	131@30	0.5	0.26
$K_2Ni_2TeO_6$[27]	65@6.4	3.825	0.25
PTCDA[28]	131@10	1.0	0.13
PAQS[29]	200@20	2	0.40
PPTS[30]	250@100	1.2	0.30
ADAPTS[23]	134@15.5	0.66	0.09
$KVPO_4F$[31]	92@6.65	4.076	0.37
KVP_2O_7[32]	60@25.4	1.3	0.08
$KVPO_4F$[33]	105@5	4.08	0.43

$KVOPO_4$[34]	115@24	2	0.23

References

1 L. Deng, T. Wang, Y. Hong, M. Feng, R. Wang, J. Zhang, Q. Zhang, J. Wang, L. Zeng, Y. Zhu and L. Guo, *ACS Energy Letters*, 2020, **5**, 1916–1922.

2 L. Deng, J. Qu, X. Niu, J. Liu, J. Zhang, Y. Hong, M. Feng, J. Wang, M. Hu, L. Zeng, Q. Zhang, L. Guo and Y. Zhu, *Nature Communications*, 2021, **12**, 2167.

3 L. Li, Z. Hu, Y. Lu, C. Wang, Q. Zhang, S. Zhao, J. Peng, K. Zhang, S.-L. Chou and J. Chen, *Angewandte Chemie International Edition*, , DOI:https://doi.org/10.1002/anie.202103475.

4 W. Ren, X. Chen and C. Zhao, *Advanced Energy Materials*, 2018, **8**, 1801413.

5 J. W. Heo, M. S. Chae, J. Hyoung and S.-T. Hong, *Inorganic Chemistry*, 2019, **58**, 3065–3072.

6 D. Su, A. McDonagh, S.-Z. Qiao and G. Wang, *Advanced Materials*, 2017, **29**, 1604007.

7 C. Li, X. Wang, W. Deng, C. Liu, J. Chen, R. Li and M. Xue, *ChemElectroChem*, 2018, **5**, 3887–3892.

8 C. Zhang, Y. Xu, M. Zhou, L. Liang, H. Dong, M. Wu, Y. Yang and Y. Lei, *Advanced Functional Materials*, 2017, **27**, 1604307.

9 G. He and L. F. Nazar, *ACS Energy Letters*, 2017, **2**, 1122–1127.

10 M. Qin, W. Ren, J. Meng, X. Wang, X. Yao, Y. Ke, Q. Li and L. Mai, *ACS Sustainable Chemistry & Engineering*, 2019, **7**, 11564–11570.

11 Y. Sun, C. Liu, J. Xie, D. Zhuang, W. Zheng and X. Zhao, *New Journal of Chemistry*, 2019, **43**, 11618–11625.

12 Q. Xue, L. Li, Y. Huang, R. Huang, F. Wu and R. Chen, *ACS Applied Materials & Interfaces*, 2019, **11**, 22339–22345.

13 Z. Shadike, D. R. Shi, Tian Wang, M. H. Cao, S. F. Yang, J. Chen and Z. W. Fu, *Journal of Materials Chemistry A*, 2017, **5**, 6393–6398.

14 X. Jiang, T. Zhang, L. Yang, G. Li and J. Y. Lee, *ChemElectroChem*, 2017, **4**, 2237–2242.

15 S. Chong, Y. Chen, Y. Zheng, Q. Tan, C. Shu, Y. Liu and Z. Guo, *Journal of Materials Chemistry A*, 2017, **5**, 22465–22471.

16 Y. Luo, B. Shen, B. Guo, L. Hu, Q. Xu, R. Zhan, Y. Zhang, S. Bao and M. Xu, *Journal of Physics and Chemistry of Solids*, 2018, **122**, 31–35.

17 P. Padigi, J. Thiebes, M. Swan, G. Goncher, D. Evans and R. Solanki, *Electrochimica Acta*, 2015, **166**, 32–39.

18 M. Morant-Giner, R. Sanchis-Gual, J. Romero, A. Alberola, L. García-Cruz, S. Agouram, M. Galbiati, N. M. Padial, J. C. Waerenborgh, C. Martí-Gastaldo, S. Tatay, A. Forment-Aliaga and E. Coronado, *Advanced Functional Materials*, 2018, **28**, 1706125.

19 J. Liao, Q. Hu, Y. Yu, H. Wang, Z. Tang, Z. Wen and C. Chen, *Journal of Materials Chemistry A*, 2017, **5**, 19017–19024.

20 S. Chong, Y. Wu, S. Guo, Y. Liu and G. Cao, *Energy Storage Materials*, 2019, **22**, 120–127.
21 B. Lin, X. Zhu, L. Fang, X. Liu, S. Li, T. Zhai, L. Xue, Q. Guo, J. Xu and H. Xia, *Advanced Materials*, 2019, **31**, 1900060.
22 H. Kim, D.-H. Seo, J. C. Kim, S.-H. Bo, L. Liu, T. Shi and G. Ceder, *Advanced Materials*, 2017, **29**, 1702480.
23 H. Kim, J. C. Kim, S.-H. Bo, T. Shi, D.-H. Kwon and G. Ceder, *Advanced Energy Materials*, 2017, **7**, 1700098.
24 J. Y. Hwang, J. Kim, T. Y. Yu, S. T. Myung and Y. K. Sun, *Energy and Environmental Science*, 2018, **11**, 2821–2827.
25 T. Deng, X. Fan, J. Chen, L. Chen, C. Luo, X. Zhou, J. Yang, S. Zheng and C. Wang, *Advanced Functional Materials*, 2018, **28**, 1800219.
26 Y.-H. Zhu, Q. Zhang, X. Yang, E.-Y. Zhao, T. Sun, X.-B. Zhang, S. Wang, X.-Q. Yu, J.-M. Yan and Q. Jiang, *Chem*, 2019, **5**, 168–179.
27 T. Masese, K. Yoshii, Y. Yamaguchi, T. Okumura, Z. D. Huang, M. Kato, K. Kubota, J. Furutani, Y. Orikasa, H. Senoh, H. Sakaebe and M. Shikano, *Nature Communications*, 2018, **9**, 3823.
28 Y. Chen, W. Luo, M. Carter, L. Zhou, J. Dai, K. Fu, S. Lacey, T. Li, J. Wan, X. Han, Y. Bao and L. Hu, *Nano Energy*, 2015, **18**, 205–211.
29 Z. Jian, Y. Liang, I. A. Rodríguez-Pérez, Y. Yao and X. Ji, *Electrochemistry Communications*, 2016, **71**, 5–8.
30 M. Tang, Y. Wu, Y. Chen, C. Jiang, S. Zhu, S. Zhuo and C. Wang, *Journal of Materials Chemistry A*, 2019, **7**, 486–492.
31 K. Chihara, A. Katogi, K. Kubota and S. Komaba, *Chemical Communications*, 2017, **53**, 5208–5211.
32 W. B. Park, S. C. Han, C. Park, S. U. Hong, U. Han, S. P. Singh, Y. H. Jung, D. Ahn, K.-S. Sohn and M. Pyo, *Advanced Energy Materials*, 2018, **8**, 1703099.
33 H. Kim, D.-H. Seo, M. Bianchini, R. J. Clément, H. Kim, J. C. Kim, Y. Tian, T. Shi, W.-S. Yoon and G. Ceder, *Advanced Energy Materials*, 2018, **8**, 1801591.
34 J. Liao, Q. Hu, B. Che, X. Ding, F. Chen and C. Chen, *Journal of Materials Chemistry A*, 2019, **7**, 15244–15251.